

Accepted Manuscript

Antibacterial activity and mechanism of action of the benzazole acrylonitrile-based compounds: *In vitro*, spectroscopic, and docking studies

Shaikha S. AlNeyadi, Alaa A. Salem, Mohammad A. Ghattas, Noor Atatreh, Ibrahim M. Abdou



PII: S0223-5234(17)30371-9

DOI: [10.1016/j.ejmech.2017.05.010](https://doi.org/10.1016/j.ejmech.2017.05.010)

Reference: EJMECH 9440

To appear in: *European Journal of Medicinal Chemistry*

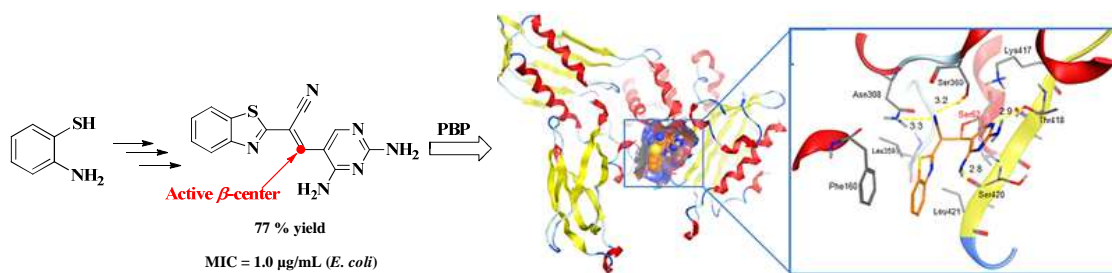
Received Date: 24 December 2016

Revised Date: 1 May 2017

Accepted Date: 2 May 2017

Please cite this article as: S.S. AlNeyadi, A.A. Salem, M.A. Ghattas, N. Atatreh, I.M. Abdou, Antibacterial activity and mechanism of action of the benzazole acrylonitrile-based compounds: *In vitro*, spectroscopic, and docking studies, *European Journal of Medicinal Chemistry* (2017), doi: 10.1016/j.ejmech.2017.05.010.

This is a PDF file of an unedited manuscript that has been accepted for publication. As a service to our customers we are providing this early version of the manuscript. The manuscript will undergo copyediting, typesetting, and review of the resulting proof before it is published in its final form. Please note that during the production process errors may be discovered which could affect the content, and all legal disclaimers that apply to the journal pertain.



The binding mode of compound 5 (ball and stick in orange) docked into the PBP binding site

Antibacterial activity and mechanism of action of the benzazole acrylonitrile-based compounds: *in vitro*, spectroscopic, and docking studies

Shaikha S. AlNeyadi^a, Alaa A. Salem^a, Mohammad A. Ghattas^b, Noor Atatreh^b and Ibrahim M. Abdou^{*a}

^a Department of Chemistry, College of Science, UAE University Al-Ain, 15551 UAE

^b College of Pharmacy, Al Ain University of Science and Technology, Al Ain, 64141 UAE

Abstract: A new series of pyrimidine derivatives **5**, **9a-d** and **12a-d** was synthesized by an efficient procedure. The antibacterial activity of the new compounds was studied against four bacterial strains. Compound **5** was found to exhibit the highest potency, with = 1.0 µg/mL, against both *Escherichia coli* and *Pseudomonas aeruginosa* when compared with amoxicillin (MIC = 1.0–1.5 µg/mL). Transmission electron microscope results confirmed that activities against bacteria occurred via rupturing of the cell wall. Molecular modeling results suggested that compounds **5**, **9a-d** and **12a-d** have the potential to irreversibly bind to the penicillin-binding protein (PBP) Ser62 residue in the active site and were able to overcome amoxicillin resistance in bacteria by inhibiting the β-lactamase enzyme. Docking studies showed that compounds **5**, **9a-d** and **12a-d** inhibit the β-lactamase enzyme through covalent bonding with Ser70. The synergistic effect with amoxicillin was studied. The newly synthesized compounds reported in this study warrant further consideration as prospective antimicrobial agents.

Keywords: pyrimidine, synthesis, antibacterial, β-lactamase, PBP, docking.

*Corresponding author.

E-mail address: i.abdou@uaeu.ac.ae (Ibrahim M. Abdou)

1. Introduction

Microbial infections are becoming the most pressing issue for global health and the economy. Therefore, intensive efforts are underway to develop new antimicrobial agents. The design of new compounds to deal with resistant bacteria has become one of the most important areas of antibacterial research today, since the resistance of pathogenic bacteria to available antimicrobial drugs is rapidly becoming a major problem worldwide. The discovery of novel and potent antibacterial agents is the greatest challenge for today's chemists and pharmacists to prevent the emergence of resistance to existing drugs. Organisms such as methicillin-resistant *Staphylococcus aureus*, vancomycin-resistant enterococci (VRE), and Gram-negative bacilli are resistant to all antibiotics used in the treatment of infections [1]. Results of bioassays and structure-activity relationship (SAR) investigations indicate that existing marketed drugs have limitations, and some have toxic side effects. An understanding of the mechanism of resistance can play a major role in developing new agents that might have better activity.

Benzimidazoles and benzothiazoles are important pharmacophores in medicinal chemistry owing to their involvement as key components for various biological activities. Benzothiazoles and their derivatives exhibit antitumor [2], antimicrobial [3], and antiviral [4] activities. Benzimidazoles have been found to display anticancer [5], antiviral [6], anti-inflammatory [7], antimicrobial [8], antioxidant [9], and anticoagulant properties [10]. Extensive biochemical and pharmacological studies have confirmed that benzimidazole and benzothiazole derivatives are effective against various strains of microorganisms. The antibacterial activities of these compounds are due to structural similarity to purine, resulting

in competitive inhibition of the synthesis of nucleic acids and proteins inside the bacterial cell wall [11]. Organic compounds containing pyrimidine scaffold as a core unit are known to exhibit various biological and pharmaceutical actions such as antiviral, antibacterial, antitumor, anti-inflammatory, and antifungal activities [12]. Considerable improvement in the biological potential and discovery of many efficacious and safer drugs was observed when two or more pharmacophores were combined together in one molecule. The hybrid molecules have the advantage of low toxicity and exhibit synergy in the medicinal efficacy of the individual moieties [13].

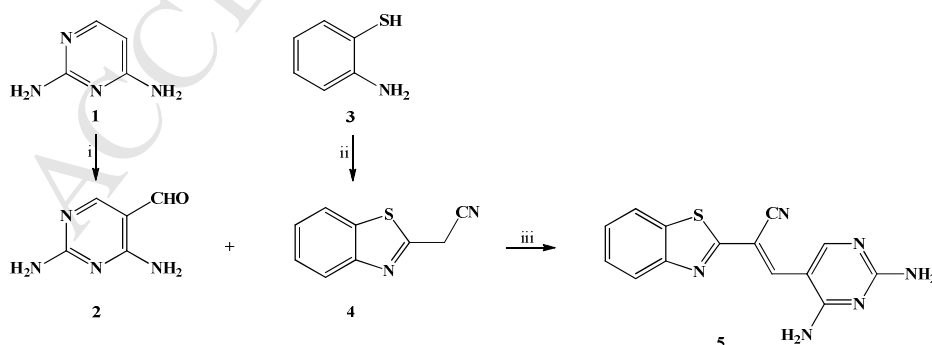
The therapeutic importance of these classes of compounds inspired us towards the development of small molecules as therapeutic agents; herein we report the design and synthesis of pyrimidine analogues containing benzimidazole and benzothiazole moieties by a simple and efficient method to evaluate the antibacterial potencies of this class of novel compounds. The synthesized compounds **5**, **9a-d** and **12a-d** were characterized by their elemental analysis, IR, and 1D-NMR spectral studies. Findings of biological activities indicate that some compounds possess potential antimicrobial activity.

2. Results and Discussion

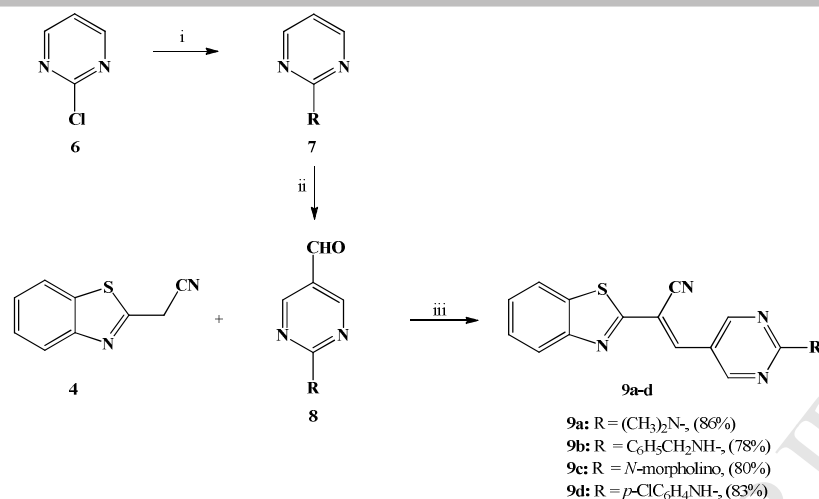
2.1. Chemistry

The synthesis of new and potentially useful compounds **5**, **9** and **12**, in which a pyrimidine ring was linked to the benzimidazole or benzothiazole moieties through an acrylonitrile bridge, was carried out by a simple and efficient synthetic procedure (Schemes 1-3). The new pyrimidines were designed by introducing an α,β -unsaturated nitrile as an active β -center to be targeted by nucleophilic residues in the enzyme's active site, and also to form additional H-bonds, resulting in new features which enhance the biological activities of the obtained products **5**, **9** and **12**.

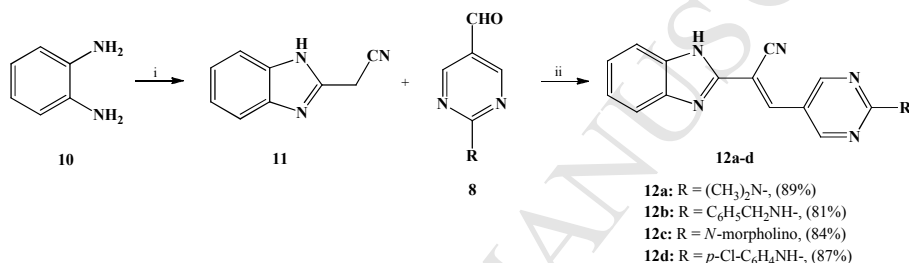
It is known that heteroaromatic nitrile derivatives undergo Knoevenagel condensation reactions with aryl aldehydes to yield 3-aryl-2-hetarylacrylonitrile derivatives [14]. In the current study, we report the synthesis of a new series of benzazole pyrimidine acrylonitriles **5**, **9a-d** and **12a-d**. A condensation between an equimolar amount of 2-benzazole acrylonitriles **4,11** and pyrimidine aldehydes **2,8** in the presence of a catalytic amount of piperidine proceeded well and gave the final products **5**, **9** and **12** in yields 77–89 %, with excellent purities (Schemes 1-3).



Scheme 1. Synthesis of (*E*)-2-(benzo[*d*]thiazol-2-yl)-3-hetarylacrylonitriles **5**: *i* = POCl₃/DMF, NaHCO₃, EtOH, 25°C, 5 h *ii* = CH₂(CN)₂, EtOH, 25°C, 5 h *iii* = piperidine, 25°C, 15 min.



Scheme 2. Synthesis of (*E*)-2-(benzo[*d*]thiazol-2-yl)-3-hetarylacrylonitriles **9**: *i* = R-NH₂, *N,N*-diisopropyl ethylamine (DIPEA), EtOH, MW, 120°C, 150 W, 10 min *ii* = POCl₃/DMF, NaHCO₃ *iii* = piperidine, 25°C, 15 min.



Scheme 3. Synthesis of (*E*)-2-(benzo[*d*]imidazol-2-yl)-3-hetarylacrylonitriles **12**: *i* = ethyl cyanoacetate, EtOH, reflux, 20 min. *ii* = piperidine, 25°C, 15 min

It seems reasonable that the condition used in this work would promote the Knoevenagel reaction through the active methylene of **4** or **11** as a precursor. The reaction begins by deprotonation of the activated methylene in the presence of a catalytic amount of piperidine. The activated methylene attacks the carbonyl carbons of the aldehydes in pyrimidines **2** or **8** to produce **5**, **9**, **12** (see Appendix A, Fig S1) [15].

All obtained compounds **5**, **9** and **12** were fully characterized using elemental analysis, FT-IR, and NMR spectroscopic techniques. Both ¹H- and ¹³C-NMR data were consistent with the presence of pyrimidine, benzothiazole, and benzimidazole moieties. The ¹H-NMR data of all derivatives revealed a single olefinic proton, consistent with the formation of a single isomer, which was assigned to be the thermodynamically more stable *E* configuration [16]. The obtained *E*-isomer is stabilized by the presence of hydrogen bonding between the olefinic proton and the imidazole nitrogen, in addition to the steric repulsions between the aromatic and heteroaromatic groups in the *Z*-conformer [17],[18].

The IR spectra of compounds **9a-d** showed characteristic absorption bands at 2010–2232 cm⁻¹ and 1565–1614 cm⁻¹ corresponding to the CN and C=C functions, respectively. In addition, it confirmed the absence of both the carbonyl group and the aldehyde proton (CHO) in the final products. The ¹H-NMR spectra for compounds **9a-d** showed that the olefinic protons were observed at very low fields within a range $\delta = 8.17$ – 8.87 ppm due to the highly deshielded protons in the *E*-form. This is one of the driving forces for greater stability and planarity for the compounds **9a-d** [19]. The ¹H-NMR spectra also demonstrated the absence of a sharp aldehyde-proton singlet at $\delta = 9.90$ ppm, confirming the formation of the targeted products **9a-d**, while the pyrimidine protons (H-4,6)

appeared within a range $\delta = 8.52\text{--}9.44$ ppm. Further ^{13}C -NMR evidence confirming the formation of a carbon-carbon double bond is the disappearance of the signal at $\delta = 22.8$ ppm, corresponding to the methylene CH_2 carbon and the appearance of the new olefinic signal. In the ^{13}C -spectra, the olefinic carbons resonated in the range of $\delta = 147.1\text{--}162.9$ ppm, and the signal appeared at $\delta = 112.2\text{--}117.4$ ppm assigned to the CN group, while the pyrimidine C4 and C6 appeared at $\delta = 152.8\text{--}164.5$ ppm. The presence of aromatic C-H, aliphatic C-H, CN, and C=C signals at 3053, 2968, 2210, and 1582 cm^{-1} , respectively, in the IR spectrum of compound **9c**, indicated the formation of the desired product. Furthermore, its ^1H -NMR spectrum recorded a singlet peak at $\delta = 8.51$ ppm, attributable to the olefinic proton, as well as retaining the morpholine ring protons appearing at $\delta = 3.67\text{--}3.68$ ppm and $\delta = 3.83\text{--}3.84$ ppm. The H_4 and H_6 of pyrimidine ring resonated as a singlet at $\delta = 8.94$ ppm. Benzimidazole-2-acetonitrile **11** is the second convenient precursor used [20],[21] in our study. Benzimidazole-2-acetonitrile **11** was allowed to react with pyrimidine aldehydes **8** in the presence of catalytic amounts of piperidine to afford (E)-2-(benzo[d]imidazol-2-yl)-3-arylacrylonitriles **12a-d** at yields of 81–89 % (Scheme 2). Structures of the obtained acrylonitrile derivatives **12a-d** were established on the basis of their elemental analysis along with their compatible spectral data. The FT-IR spectra of compounds **12b** showed characteristic absorption bands at 2207 cm^{-1} , 1604 cm^{-1} , and 3439 cm^{-1} corresponding to the CN, C=C and NH- groups, respectively. The ^1H -NMR spectrum indicated the presence of a low-field olefinic proton in the region of $\delta = 8.46\text{--}8.88$ ppm accounting for the formation of target compound **12b**. In addition, the docking study and energy minimization supported the formation of the *E*-isomer, with a potential energy of 11.83 kcal/mol compared with 12.66 kcal/mol for the *Z*-isomer.

2.2. Biological Studies

2.2.1. Antimicrobial activity

Biological activities of compounds containing pyrimidine rings have stimulated considerable interest in exploring the synthesis of new and potentially useful compounds. Novel derivatives **5**, **9a-d** and **12a-d** were evaluated for their *in-vitro* antibacterial activity against two Gram-positive bacterial strains, namely, *Staphylococcus aureus* (ATCC-25923) and *Bacillus subtilis* (ATCC 6633); and two Gram-negative bacterial strains, namely, *Escherichia coli* (ATCC-25922) and *Pseudomonas aeruginosa* (ATCC-27853) using the well diffusion method. Amoxicillin was used as the reference standard. The results of screening derivatives **5**, **9a-d** and **12a-d** are summarized in Table 1. Among the series, two compounds, **5** and **12d**, exhibited excellent antibacterial activity against both Gram-positive and Gram-negative bacteria with a MIC ranging from 1 to 13 $\mu\text{g/mL}$. Compounds **9a**, **9d**, **12b**, and **12a** exhibited moderate antibacterial activity against the tested organisms (MIC = 11.1 to 25 $\mu\text{g/mL}$). However, all other compounds in the series were found to have good activity against both Gram-positive and Gram-negative bacteria, as compared to amoxicillin. The *in-vitro* antibacterial screening of compounds **5**, **9a-d** against *E. coli* showed that compound **5** (MIC = 1.0 $\mu\text{g/mL}$) exhibited slightly higher antibacterial activity than the control (amoxicillin, MIC = 1.5 $\mu\text{g/mL}$), whereas compound **12d** had an MIC value of 9.0 $\mu\text{g/mL}$. The remaining compounds showed good activity against *E. coli* with MIC values between 11.1 and 50 $\mu\text{g/mL}$, compared with amoxicillin 1.5 $\mu\text{g/mL}$. Compounds **5**, **9** and **12**

were found to inhibit *S. aureus* at MIC values between 8.0 and 35.8 $\mu\text{g/mL}$. In addition, compounds **5** and **12d** exhibited good antimicrobial activities, compared with amoxicillin (MIC = 1.5 $\mu\text{g/mL}$), against Gram-positive *Bacillus subtilis* bacteria, with MIC ranging between 8.0-13.0 $\mu\text{g/mL}$ (Table 1), (Fig. 1). Therefore, the biological results obtained for the new pyrimidine analogues **5**, **9d**, and **12d** showed promising antibacterial activity against Gram-positive and Gram-negative bacteria (Table 1). A brief investigation of the structure-activity relationship (SAR) revealed that halogen substitution at the pyrimidine ring contributed to better antibacterial activity. Furthermore, the presence of amino groups at positions 2- and 4- of the pyrimidine ring improved the antibacterial properties. It has been reported that fusing two biodynamic heteroaryl systems can result in the formation of a new scaffold with significant biological activity [22]. In addition, the linkage of pyrimidine to benzothiazole or benzimidazole was found to enhance the antibacterial activities of the final products. Results presented in Table 1 indicate that all the tested compounds exhibited greater activity against Gram-positive and Gram-negative bacteria strains than amoxicillin, while the benzimidazole analogues exhibited more potent activity than the benzothiazole derivatives.

Table 1

Agar well diffusion method – zone of inhibition and MIC ($\mu\text{g/ml}$) of pyrimidines **5**, **9a–d** and **12a–d**.

Compounds	Zone of inhibition (mm)				MIC ($\mu\text{g/ml}$)			
	<i>E. coli</i>	<i>P. aeruginosa</i>	<i>S. aureus</i>	<i>B. subtilis</i>	<i>E. coli</i>	<i>P. aeruginosa</i>	<i>S. aureus</i>	<i>B. subtilis</i>
5 	47	28	32	40	1.0	1.0	8.0	8.0
9a 	52	32	35	45	50	35.8	35.8	50
9b 	50	35	35	39	18.3	18.3	18.3	18.3
9c 	40	30	32	39	35.8	35.8	27.8	50
9d 	40	30	30	35	11.1	11.1	11.1	20
12a 	50	30	30	39	14.3	11.1	11.1	20
12b 	45	30	35	40	18	18	18	25
12c 	40	35	35	39	27.8	27.8	27.8	27.8
12d 	40	28	32	40	9.0	9.0	9.0	13
Amoxicillin 	21	24	25	14	1.5	1	1.5	1.5

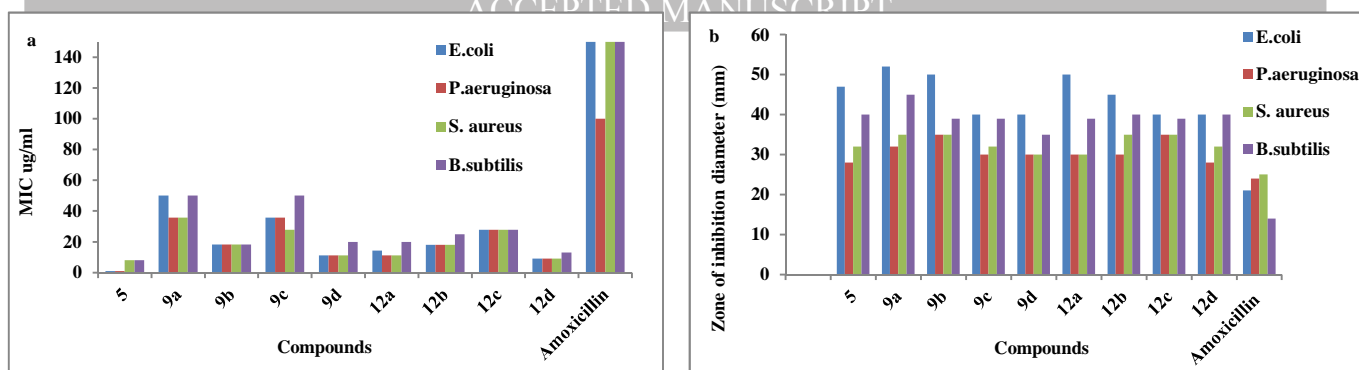


Fig. 1. a) A plot of the minimum inhibitory concentration ($\mu\text{g/ml}$) for four strains of bacteria; b) Zone of inhibition areas of the new pyrimidines **5**, **9** and **12** compared with amoxicillin.

2.2.2. Investigation of *in-vitro* amoxicillin combined with compound **5** or **12d**

Antibiotic combinations are used to enhance antibacterial efficacy and to prevent the development of resistance. Antibiotic combinations are frequently used in order to obtain broad-spectrum effects in the treatment of serious infections such as septicemia and endocarditis, and also to produce an *in-vivo* effect against strains which are defined as resistant to the known inhibiting or fatal dose of one antibiotic [23].

Certain combinations of β -lactam antibiotics exhibit synergistic antibacterial effects against various strains. Amoxicillin is similar to penicillin in its bactericidal action against susceptible bacteria during the stage of active multiplication. It acts through the inhibition of cell wall biosynthesis, leading to the death of the bacterium. Its usefulness is limited by its susceptibility to β -lactamase enzyme hydrolysis produced by the organism [24].

The synergistic effects of combinations such as (amoxicillin + **5**) and (amoxicillin + **12d**) were studied. Equal volumes of amoxicillin (MIC) with **5** (MIC), and **12d** with amoxicillin were mixed. A $1.0 \mu\text{g/ml}$ concentration of amoxicillin was mixed with a $13.0 \mu\text{g/ml}$ concentration of **12d** and made up to a range of dilutions (100, 80, 60, 40, 10, and 5 %). Thereby, the 100 % dilution will contain amoxicillin $1.0 \mu\text{g/ml}$ and **12d** MIC $13.0 \mu\text{g/ml}$, and 10 % will contain amoxicillin $0.1 \mu\text{g/ml}$ and **12d** $1.3 \mu\text{g/ml}$ (Tables 2, 3 and Fig. 2).

Table 2MIC for amoxicillin (MIC) with **5** and **12d** (MIC).

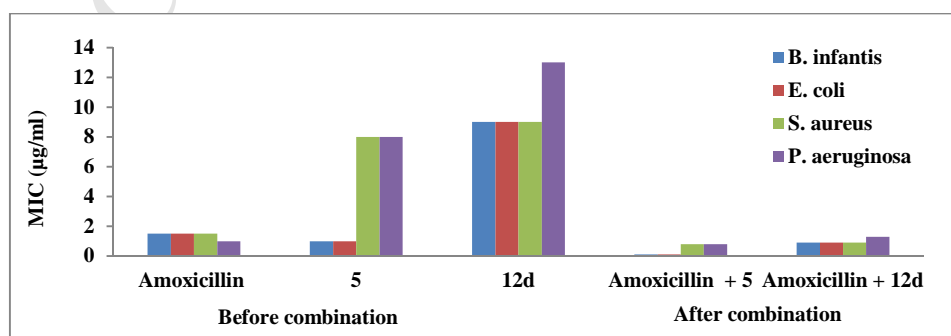
S. No	Dilution (%)	<i>B. infantis</i> (10 ⁵ cells/ml)		<i>E. coli</i> (10 ⁵ cells/ml)		<i>S. aureus</i> (10 ⁵ cells/ml)		<i>P. aeruginosa</i> (10 ⁵ cells/ml)	
		A+ 5	A+ 12d	A+ 5	A+ 12d	A+ 5	A+ 12d	A+ 5	A+ 12d
1	100	N	N	N	N	N	N	N	N
2	80	N	N	N	N	N	N	N	N
3	60	N	N	N	N	N	N	N	N
4	40	N	N	N	N	N	N	N	N
5	10	N	N	N	N	N	N	N	N
6	05	G	G	G	G	G	G	G	G
7	+ve control	G	G	G	G	G	G	G	G
8	-ve control	N	N	N	N	N	N	N	N

Note: A: amoxicillin; N: no growth; G: bacterial growth; +ve control: bacteria with only nutrient broth (to check if bacteria grown or not); -ve control: sterile nutrient broth (to check contamination).

Table 3

Activities of compounds **5** and **12d** (MICs) and the combination of amoxicillin with **5** and amoxicillin with **12d** against bacteria strains.

Bacteria	Amoxicillin MIC (µg/ml)	5 MIC (µg/ml)	12d MIC (µg/ml)	MIC (µg/ml) of amoxicillin + 5	MIC (µg/ml) of amoxicillin + 12d
<i>B. infantis</i>	1.5	1.0	9.0	0.1	0.9
<i>E. coli</i>	1.5	1.0	9.0	0.1	0.9
<i>S. aureus</i>	1.5	8.0	9.0	0.8	0.9
<i>P. aeruginosa</i>	1.0	8.0	13.0	0.8	1.3

**Fig. 2.** Activities of pyrimidine acrylonitrile derivatives **5**, **12d**, and amoxicillin (MICs) before and after combination.

Synergistic effects can be clearly observed from Table 3. We can see that in the case of *E. coli*, promising antibacterial activity is obtained for the amoxicillin combinations, whereas for the amoxicillin alone less activity is observed.

Synergy has been defined as requiring a fourfold reduction in the MIC of both antibiotics in combination, compared with each one being used alone, measuring the fractional inhibitory concentration index (FICI). The FICI was calculated for each combination (**5** + amoxicillin and **12d** + amoxicillin) using the following formula [25]:

$$FICI = \frac{MIC_{5 \text{ or } 12d}(\text{combination})}{MIC_{5 \text{ or } 12d}(\text{alone})} + \frac{MIC_{\text{Amoxicillin}}(\text{Combination})}{MIC_{\text{Amoxicillin}}(\text{alone})}$$

The FICI was interpreted as follows: synergistic, $FICI \leq 0.5$; additive, $0.5 < FICI \leq 1$; indifferent, $1 < FICI \leq 2$; antagonistic, $FICI > 2$.

The FICI values for the two combinations of (**5** + amoxicillin) and (**12d** + amoxicillin) were 0.2, indicating synergy. The synergy between **5** and **12d** and amoxicillin has been attributed to the increase in the uptake of compounds **5** and **12d**. The compounds **5** and **12d** are resistant to hydrolysis by the β -lactamase enzyme elaborated by the strain of organism being tested. Compounds **5** and **12d** seem to act not only as antibacterial agents, but also may act as β -lactamase inhibitors, preventing bacterial degradation of amoxicillin. Thus, the synergistic effect on the MIC of the mixture is more effective than applying amoxicillin alone. The combination also allows lower doses of both amoxicillin and compounds **5** or **12d** to be used, helping to reduce toxicity, broadening the empiric coverage provided by the two antimicrobial agents (with different spectra of activity), and preventing or delaying the emergence of resistance during antimicrobial therapy.

2.3. Docking Study

2.3.1. Penicillin-binding protein

The novel pyrimidine acrylonitrile derivatives have an α,β -unsaturated nitrile that can be easily attacked by a nucleophile. Similar acrylonitrile-based compounds showed time-dependent inhibition for the botulinum neurotoxin serotype A metalloprotease enzyme [26], suggesting the formation of a covalent bond between its acrylonitrile group and an allosteric site cysteine residue. Hence, it might be sensible to suggest that our compounds can also inhibit the target enzyme in an irreversible manner (Fig. 3).

One of the most well-known bacterial targets for irreversible inhibitors is the penicillin-binding protein (PBP), which could be a target for our benzazole acrylonitriles. To study whether that is theoretically possible, our compounds were covalently docked into the *E. coli* PBP active pocket. The resultant docking affinities showed favorable binding modes for all docked compounds (Table 4), where all ligands had scores between -3.0 and -4.0 kcal/mol. Compound **5** achieved the lowest docking score amongst all synthesized compounds, which was in line with the experimental antimicrobial results.

The reference compound, amoxicillin, used in the experiment was also docked into the PBP active site and obtained a minimum energy of -6.2 kcal/mol (Table 4). In contrast to the *in silico* results obtained, the pyrimidine acrylonitrile derivatives **5**, **9** and **12** showed better *in-vitro* antimicrobial activity than amoxicillin. This can be explained by the poor correlation between predicted binding energies and the corresponding experimental affinities scoring functions [27].

The docked binding mode of **5** shows how the ligand (nitrile-activated) double bond formed a covalent interaction with the nucleophilic residue in the PBP active site Ser62 (Fig. 4). As for the non-covalent interactions stabilizing the **5**-PBP complex, the cyano group nitrogen seems to be involved in two possible electrostatic interactions with the side chains of Asn308 and Ser360. The pyrimidine nitrogen's presence in compound **5** allowed the formation of additional hydrogen bond with the hydroxyl group of Thr418, whilst the aromatic amine side chain allowed further hydrogen bond with the backbone amide of Ser420. Moreover, the benzothiazole ring was docked into a hydrophobic pocket, creating a π - π stacking interaction with the aromatic ring of Phe160 and multiple van der Waals interactions with the side chains of Leu359 and Leu421, providing further stabilization for the ligand-receptor complex (Fig. 4).

Overall, the newly synthesized compounds **5**, **9** and **12** appear to have the major features required to enter the PBP catalytic pocket and irreversibly occupy it. The formation of the covalent complex suggested that the enzyme would be permanently damaged, resulting in cell wall synthesis inhibition. Indeed, further work is required to confirm that the PBP enzyme is a target for our novel antibacterial agents.

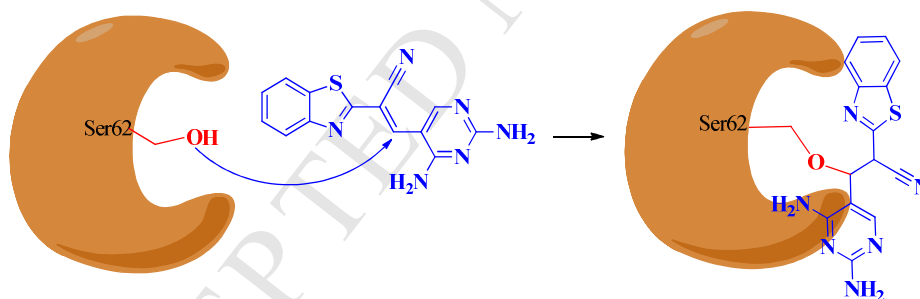


Fig. 3. The proposed mechanism of PBP inhibition by the acrylonitrile-based compounds.

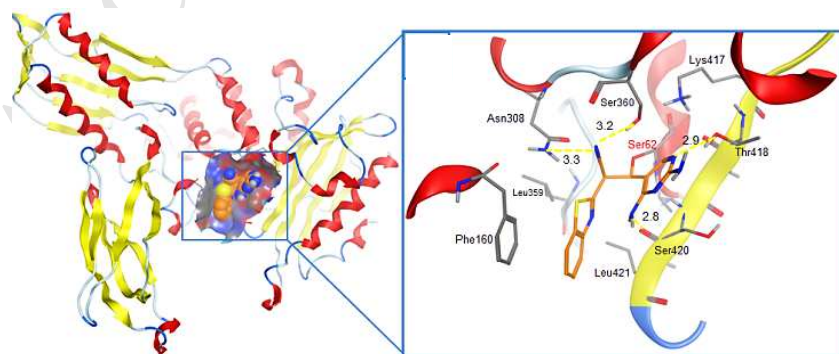


Fig. 4. The binding mode of compound **5** (ball and stick in orange) docked into the PBP binding site (surrounding residues shown as gray sticks). The nucleophilic residue is labeled in red. The picture was generated by MOE [28]. Hydrogen bonding is shown as yellow dotted lines with distances in angstrom.

Table 4

Docking affinities obtained from covalent docking of acrylonitrile-based antibacterial agents into the *E. coli* PBP active site and from experimentally testing them against *E. coli*.

Compound No.	Docking affinity (kcal/mol)
5	-4.0
12d	-3.3
Amoxicillin	-6.2

2.3.2. β -Lactamase enzyme

It was found that a similar class of compounds showed time-dependent inhibition of the botulinum neurotoxin serotype A metalloprotease enzyme through the formation of a covalent interaction between their acrylonitrile group and an allosteric site cysteine residue [26]. To further investigate the action of the newly synthesized benzazole derivatives as antimicrobial active compounds, an experiment was designed to study the possible mode of interaction with the β -lactamase enzyme (Fig. 5). Consequently, a theoretical study was undertaken to evaluate the possibility of a covalent interaction with the *E. coli* β -lactamase active pocket. The docking affinity results showed stable binding energies for all docked compounds ranging between -4.2 and -6.3 kcal/mol (Table 5).

The ligand **5** appears to fit in the β -lactamase pocket very nicely, explaining how this ligand was able to obtain a minimum binding energy of -5.9 kcal/mol (Fig. 6). This was probably attributed to the hydrogen bonding formed between the **5** cyanide and the Ser130 side chain; positioning the nitrile-activated double bond to form a covalent bond with the Ser70 hydroxyl group. Additionally, the 2-amino group of the pyrimidine ring formed a hydrogen bond with the hydroxyl group of Ser235. Thus, these compounds can irreversibly bind the β -lactamase enzyme. Further *in-vitro* testing is required, however, to confirm that Ser70 is the site of reaction for compounds **5**, **9** and **12**.

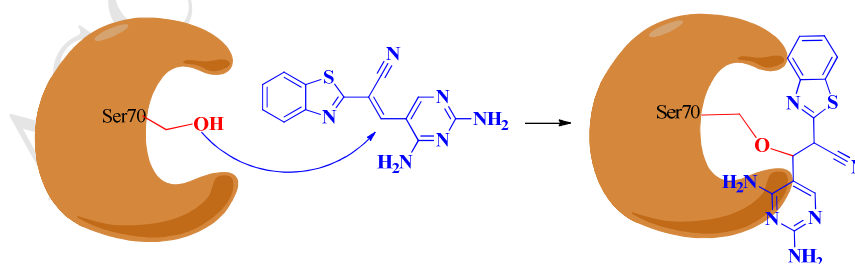


Fig. 5. The proposed mechanism of inhibition of the β -lactamase enzyme by **5**.

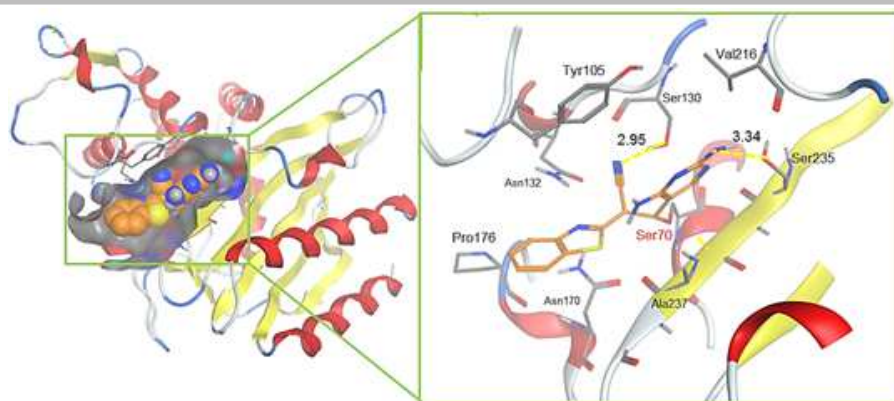


Fig. 6. The binding mode of **5** (ball and stick in orange) docked into the β -lactamase pocket (surrounding residues shown as gray sticks). The nucleophilic residue is labeled in red. The picture was generated by MOE [28]. Hydrogen bonding is shown as yellow dotted lines with distance in angstrom.

Table 5

Docking affinities obtained from covalent docking of compounds **5**, **9** and **12** into the *E. coli* β -lactamase active site.

Compound No.	Docking Affinity (kcal/mol)
5	-5.9
9a	-4.4
9b	-4.4
9c	-4.5
9d	-4.9
12a	-4.4
12b	-4.6
12c	-4.2
12d	-6.3

2.4. Biophysical studies

To confirm the results obtained from the *in-vitro* antimicrobial and docking studies, the interactions between the benzazole-pyrimidines **5** and **12d** and the β -lactamase enzyme were investigated using UV-vis absorption, fluorescence, circular dichroism, ^1H NMR, and SEM techniques.

2.4.1. UV-vis study

UV-vis absorption technique is a simple operational method to validate the structural change in an enzyme and to identify complex formation. In the binding experiment, UV-vis absorption spectroscopy was adopted to evaluate the binding behavior between compound **5** and the β -lactamase enzyme. The band at 280 nm was attributed to the $n\text{-}\sigma^*$, while the band at 330 nm appeared to be a combination of $n\text{-}\pi^*$ and $\pi\text{-}\pi^*$ transitions. The

β -lactamase enzyme band at 275 nm clearly interfered with the absorption band of compound **5** at 280 nm. The intensity of the band at 280 nm increased, probably because of overlapping with the β -lactamase enzyme band at 275 nm. In contrast, with the addition of compound **5**, the peak intensity of the band at 330 nm increased, indicating that compound **5** interacted with the β -lactamase enzyme (see Appendix A, Fig. S2).

The UV-spectra of compound **12d** showed two absorption bands at $\lambda = 287$ and 336 nm (see Appendix A, Fig. S3). The band at $\lambda = 287$ nm was attributed to the n- σ^* , while the band at $\lambda = 336$ nm is a combination of n- π^* and π - π^* transitions. The β -lactamase enzyme demonstrated one absorption band at $\lambda = 275$ nm and clearly interfered with the absorption band at $\lambda = 287$ nm of **12d**. Therefore, the absorbance at $\lambda = 287$ nm increased upon the addition of the β -lactamase enzyme. The intensity of the band at $\lambda = 336$ nm also increased upon the addition of the enzyme which might indicate an interaction between the enzyme and the ligand.

2.4.2. Fluorescence study

Fluorescence spectroscopy was the second method used to confirm the interaction between the active benzazole-pyrimidines **5** and **12d** and the β -lactamase enzyme in phosphate buffer, pH 7.4. The fluorescence spectrum of compound **5**, using excitation λ_{max} of 280 nm, showed an emission band at $\lambda = 443$ nm attributed to the n- π^* singlet-singlet transition. Upon sequential additions of the β -lactamase enzyme, this band had a slight red shift (~ 2 nm) with an increased intensity, indicating that compound **5** interacted with the β -lactamase enzyme. The same result was observed when compound **12d** was used in titration with β -lactamase (see Appendix A, Fig. S4).

2.4.3. Circular dichroism (CD) study

Circular dichroism (CD) is a spectroscopic technique where the absorption of molecules is measured over a range of wavelengths. CD spectroscopy is used extensively to study chiral molecules of all types and sizes. A primary use is to analyze the secondary structure and the conformation of macromolecules, such as protein secondary structures, which are found to be more sensitive to the environment. Structures change on interaction with other molecules and can be detected and studied using CD spectroscopy [29]. We conducted CD titration experiments to get more information on the interactions between compounds **5**, **9** and **12** with β -lactamase and conformation changes upon interaction. The CD spectrum of the β -lactamase enzyme in phosphate buffer at pH 7.4 showed a negative band centered at 220 nm and one positive band at 270 nm. This finding is consistent with previously reported works [30] (see Appendix A, Fig. S5).

Additions of compound **5** to the β -lactamase enzyme resulted in CD spectral changes. The intensities of the band centered at 220 nm became more positive upon the addition of compound **5**, while after extensive addition of **5**, the negative band at 220 nm blue-shifted slightly and gradually transformed into a positive band centered at 215 nm. The transformation of the negative band at 220 nm into the positive one at 215 nm indicates a change in the β -lactamase enzyme conformation upon interaction with **5**. The same results were obtained when **12d** was used, as can be seen in Appendix A, Fig. S6.

2.4.4. NMR studies: Complexation of β -lactamase with benzazole-pyrimidine **12d**

The docking studies demonstrated that the nitrile-activated double bond in compound **12d** was able to form a covalent bond with the Ser70 residue in the β -lactamase pocket. NMR was used to confirm the formation of the covalent bond between the benzazole-pyrimidine **12d** and the β -lactamase active site.

The complexation behavior of the synthesized benzazole-pyrimidine **12d** with β -lactamase enzyme was investigated as induced chemical shifts of the benzazole-pyrimidine protons. Upon addition of β -lactamase enzyme, no significant changes occurred in the chemical shifts of the benzazole-pyrimidine protons. After 60 min, the chemical shifts of the benzazole-pyrimidine protons of **12d** were observed in the upfield region. The $\Delta\delta$ calculated suggested that β -lactamase enzyme preferentially encapsulates the benzazole-pyrimidine **12d** moiety. The inclusion of compound **12d** into the β -lactamase enzyme active site led to a significant shift of the pyrimidine H-4 and H-6 to a higher field of 0.95 ppm. The disappearance of the olefinic proton of **12d** at $\delta = 7.78$ ppm and the appearance of a new signal resonance at $\delta = 5.28$ ppm integrated to one proton and assigned for the methine proton confirmed the formation of a new covalent bond in the β -lactamase pocket (see Appendix A, Fig. S7).

2.4.5. Morphological changes of *E. coli* bacteria upon the addition of compound **5**

The morphological effect observed using TEM provided evidence for interactions with, and disruption of, the cell wall. For instance, PBP located in the cytoplasmic membrane, may bind to compound **5** and changes the cell morphology which could result in PBP-compound **5** interaction. Additionally, untreated cells must be studied by electron microscopy as controls (untreated bacteria) to confirm observed changes in the bacterial cells exposed to compound **5**.

TEM analysis of unstained bacteria showed normal external morphological features of the bacterial strain. *E. coli* cells diluted in phosphate buffer exhibited many filaments, such as flagella and fimbriae (see Appendix A Fig. S8a–c). The fimbriae measured approximately 7.00 nm wide, and up to 900 nm long. In contrast, after treatment with compound **5** for 2 h the bacterial cells appeared to be seriously damaged (see Appendix A, Fig. S8d–i). The cells demonstrated unusual morphology of being cracked and ruptured. Electron-dense particles or precipitates were also observed around damaged bacterial cells. Damaged cells showed either localized or complete separation of the cell membrane from the cell wall. The cellular degradation was also accompanied by electron-translucent cytoplasm and cellular disruption in the damaged cells. These findings support the previously mentioned theory that compounds **5**, **9** and **12** could exert their antibacterial activity via inhibiting penicillin-binding protein, which is essential for bacterial cell wall synthesis.

3. Conclusion

A new series of nine benzimidazole and benzothiazole pyrimidines **5**, **9** and **12** were synthesized via an environmentally friendly and efficient procedure, and the products were then screened for their antimicrobial activities. Among the newly synthesized derivatives, compound **5** exhibited the highest antibacterial activities, which were comparable to those of the test control, amoxicillin. The bactericidal activity of these compounds was proposed, by docking, to result from the irreversible inhibition of PBP, which is important for cell wall synthesis.

In line with the *in silico* data, TEM studies showed that these compounds can cause bacterial cell wall rupture. Furthermore, these compounds exhibited the potential to overcome bacterial resistance by demonstrating significant synergism when combined with amoxicillin. Docking studies showed that these compounds have the ability to covalently bind the β -lactamase enzyme via forming an irreversible interaction with the key amino acid residue Ser62. The results obtained were confirmed using $^1\text{H-NMR}$, UV, fluorescence, and TEM techniques.

Therefore, these compounds open new avenues for the development of anti-bacterial therapeutic agents for the treatment of infectious diseases. In addition, these results give an insight into structure-activity relationships, which are tremendously important for the design of further new antimicrobial compounds.

4. Experimental

4.1. Chemistry

All reagents and chemicals were purchased from Sigma-Aldrich and used without further purification. Thin-layer chromatography (TLC) was performed on silica gel glass plates (Silica gel, 60 F₂₅₄, Fluka) and the spots were visualized under a UV lamp. Column chromatography was performed on a Kieselgel S (silica gel S, 0.063–0.1 mm). The melting points were recorded on a Gallenkamp apparatus and are uncorrected. Infrared spectra were measured using KBr pellets on a Thermo Nicolet model 470 FT-IR spectrophotometer. $^1\text{H-NMR}$ spectra were recorded on Varian, 400 MHz instruments by using DMSO-*d*₆ and CDCl₃ solutions and tetramethylsilane (TMS) as an internal reference. The element analysis was performed on a Euro Vector EA 3000. Fluorescence measurements were conducted inside quartz cells using a Cary Eclipse model-3 spectrofluorometer equipped with a high-intensity Xenon flash lamp and 1.0 cm path length (Varian, Austria). Absorption measurements were carried out using an Agilent 8453 spectrophotometer supported by 1.0 cm quartz cells (Austria). CD measurements were made using a Jasco J-815 spectrometer (Jasco, USA). A detailed description of the morphology was obtained by transmission electron microscopy (TEM; CM10-Phillips Amsterdam, Netherlands).

4.2. Amination

Compounds **7a-d** obtained by the reaction between 2-chloropyrimidine **6** (1.0 mmol, 0.148g) with the appropriate amines (1.0 mmol) in ethanol (2-3 ml) at 0°C in the presence of *N,N*-diisopropyl ethylamine (DIPEA, 1.1 mmol) under microwave irradiation for 10 min. The progress of reaction was monitored by TLC. Ethyl acetate (10.0 ml) was added to the reaction mixture and the pH was adjusted to 7-7.5 using HCl (6.0 M). The mixture was washed with saturated aqueous solution of NaHCO₃. The organic layer was dried over anhydrous MgSO₄. The excess solvent was removed under reduced pressure and the obtained residue was further purified by column chromatography using ethyl acetate-hexane (1:1) to afford the final products in good yields.

4.2.1. *N,N*-dimethylpyrimidin-2-amine (**7a**). $^1\text{H-NMR}$ [DMSO-*d*₆, 400 MHz]: (δ , ppm) 3.18 (s, 6H, CH₃), 6.85 (m, 1H, H₅-pyrimidine), 8.70 (s, 2H, H_{4,6}-pyrimidine); $^{13}\text{C-NMR}$ [DMSO-*d*₆, 100 MHz]: (δ , ppm) 37.6 (CH₃), 117.4 (C5-pyrimidine), 159.8 (C4,6-pyrimidine), 161.9 (C2-pyrimidine).

4.2.2. *N*-benzylpyrimidin-2-amine (**7b**). ¹H-NMR [DMSO-*d*₆, 400 MHz]: (δ, ppm) 4.56 (d, 2H, Ph-CH₂, *J* = 4.0 Hz), 6.68 (m, 1H, H₅-pyrimidine), 7.21-7.28 (m, 5H, aromatic), 8.69 (s, 2H, H_{4,6}-pyrimidine), 8.82 (s, 1H, NH, exchanges with D₂O); ¹³C-NMR [DMSO-*d*₆, 100 MHz]: (δ, ppm) 44.3 (CH₂, benzylamine), 119.4 (C5-pyrimidine), 127.0, 127.3, 128.5, 138.7 (aromatic), 159.2 (C4,6-pyrimidine), 160.3 (C2-pyrimidine).

4.2.3. 4-(pyrimidin-2-yl)morpholine (**7c**). ¹H-NMR [DMSO-*d*₆, 400 MHz]: (δ, ppm) 3.62-3.64 (m, 4H, morpholine), 3.84-3.85 (m, 4H, morpholine), 6.70 (m, 1H, H₅-pyrimidine), 8.72 (s, 2H, H_{4,6}-pyrimidine); ¹³C-NMR [DMSO-*d*₆, 100 MHz]: (δ, ppm) 45.1 (morpholine), 66.6 (morpholine), 119.0 (C5-pyrimidine), 159.2 (C4,6-pyrimidine), 160.1 (C2-pyrimidine).

4.2.4. *N*-(4-chlorophenyl)pyrimidin-2-amine (**7d**). ¹H-NMR [DMSO-*d*₆, 400 MHz]: (δ, ppm) 6.71 (m, 1H, H₅-pyrimidine), 7.53-7.55 (d, 2H, *p*-chlorophenyl, *J* = 8.0 Hz), 8.34 (s, 1H, NH, exchanges with D₂O), 8.40-8.41 (d, 2H, *p*-chlorophenyl, *J* = 8.0 Hz), 9.23 (s, 2H, H_{4,6}-pyrimidine); ¹³C-NMR [DMSO-*d*₆, 100 MHz]: (δ, ppm) 125.2 (C5-pyrimidine), 129.4, 129.9, 134.8, 137.5 (aromatic), 158.1 (C4,6-pyrimidine), 162.3 (C2-pyrimidine).

4.3. General synthetic procedure for formulation of pyrimidines **2** and **8**

Vilsmeier reagent was prepared by mixing ice-cold dry DMF (50 ml) and POCl₃ (30.0 mmol, 2.8 ml). The mixture was stirred for 15 min at °25C. To the previous mixture, aminopyrimidines (10.0 mmol) in dry DMF (5.0 ml) were added over a period of 15 min at 0–5 °C. The reaction mixture was stirred for 24 h at °25C. The mixture was then added to cold, saturated aq. K₂CO₃ and extracted with diethyl ether. The organic layer was washed with water, dried over anhydrous Na₂SO₄, and evaporated under reduced pressure to afford the crude product, which was purified in a silica gel column chromatography using hexane/ethyl acetate (9:1) as an eluent to give the title compounds **2** and **8**

4.3.1. 2,4-Diaminopyrimidine-5-carbaldehyde (**2**). Brown powder, yield 59 %; ¹H-NMR [DMSO-*d*₆, 400 MHz]: (δ, ppm) 7.10 (d, 2H, NH₂, exchange with D₂O), 7.52 (d, 2H, NH₂, exchange with D₂O), 8.32 (s, 1H, H₆-pyrimidine), 9.45 (CHO); ¹³C-NMR [DMSO-*d*₆, 100 MHz]: (δ, ppm) 106.2 (C5-pyrimidine), 162.7 (C4-pyrimidine), 164.4 (C6-pyrimidine), 167.0 (C2-pyrimidine), 189.5 (CHO).

4.3.2. 2-(*N,N*-Dimethylamino)pyrimidine-5-carbaldehyde (**8a**). Pale yellow crystals, yield 62 %; ¹H-NMR [DMSO-*d*₆, 400 MHz]: (δ, ppm) 3.19 (s, 6H, CH₃), 8.73 (s, 2H, H_{4,6}-pyrimidine), 9.71 (s, 1H, CHO); ¹³C-NMR [DMSO-*d*₆, 100 MHz]: (δ, ppm) 37.4 (CH₃), 119.4 (C5-pyrimidine), 160.7 (C4,6-pyrimidine), 162.8 (C2-pyrimidine), 189.2 (CHO).

4.3.3. 2-(*N*-Benzylamino)pyrimidine-5-carbaldehyde (**8b**). Yellow powder, yield 70 %; ¹H-NMR [DMSO-*d*₆, 400 MHz]: (δ, ppm) 4.57 (d, 2H, Ph-CH₂, *J* = 4.0 Hz), 7.20–7.28 (m, 5H, aromatic), 8.71 (s, 2H, H_{4,6}-pyrimidine), 8.84 (s, 1H, NH, exchanges with D₂O), 9.68 (CHO); ¹³C-NMR [DMSO-*d*₆, 100 MHz]: (δ, ppm) 44.5 (CH₂,

benzylamine), 120.7 (C5-pyrimidine), 127.3, 127.5, 128.8, 139.5 (aromatic), 160.8 (C4,6-pyrimidine), 163.8 (C2-pyrimidine), 189.1 (CHO).

4.3.4. 2-(*N*-Morpholino)pyrimidine-5-carbaldehyde (**8c**). Pale yellow powder, yield 60 %; ¹H-NMR [DMSO-*d*₆, 400 MHz]: (δ, ppm) 3.62–3.64 (m, 4H, morpholine), 3.84–3.85 (m, 4H, morpholine), 8.77 (s, 2H, H_{4,6}-pyrimidine), 9.73 (s, 1H, CHO); ¹³C-NMR [DMSO-*d*₆, 100 MHz]: (δ, ppm) 44.5 (morpholine), 66.3 (morpholine), 120.1 (C5-pyrimidine), 160.9 (C4,6-pyrimidine), 162.1 (C2-pyrimidine), 189.2 (CHO).

4.3.5. 2-(4'-Chlorobenzylamino)pyrimidine-5-carbaldehyde (**8d**). Pale yellow powder, yield 61 %; ¹H-NMR [DMSO-*d*₆, 400 MHz]: (δ, ppm) 7.58–7.60 (d, 2H, *p*-chlorophenyl, *J* = 8.0 Hz), 8.35 (s, 1H, NH, exchanges with D₂O), 8.41–8.43 (d, 2H, *p*-chlorophenyl, *J* = 8.0 Hz), 9.28 (s, 2H, H_{4,6}-pyrimidine), 10.10 (CHO); ¹³C-NMR [DMSO-*d*₆, 100 MHz]: (δ, ppm) 127.3 (C5-pyrimidine), 129.6, 130.8, 135.4, 137.6 (aromatic), 159.3 (C4,6-pyrimidine), 165.6 (C2-pyrimidine), 191.3 (CHO).

4.4. Synthesis of benzothiazole-pyrimidines

4.4.1. 2-(Benzo[*d*]thiazol-2'-yl)acetonitrile (**4**). A mixture of 2-aminothiophenol **3** (0.01 mol, 1.1 ml) and malononitrile (0.01 mol, 0.64 ml) in ethanol (10 ml) was stirred at °25C for 5 h. The yellow solid was collected by filtration and recrystallized from ethanol to give light brown crystals; yield 86 %; mp 102 °C; ¹H-NMR [DMSO-*d*₆, 400 MHz]: (δ, ppm) 4.72 (s, 2H, CH₂), 7.45–7.52 (m, 2H, H_{5,6}-benzothiazole), 8.00–8.10 (m, 2H, H_{4,7}-benzothiazole); ¹³C-NMR [DMSO-*d*₆, 100 MHz]: (δ, ppm) 22.8 (CH₂), 117.5 (CN), 122.8 (C7-benzothiazole), 123.1 (C4-benzothiazole), 126.1 (C5-benzothiazole), 127.0 (C6-benzothiazole), 135.5 (C3'a-benzothiazole), 152.7 (C3'b-benzothiazole), 161.0 (C2-benzothiazole).

4.4.2. General synthetic procedure of (E)-2-(Benzo[*d*]thiazol-2'-yl)-3-arylacrylonitriles **5** and **9a–d**

A mixture of 2-(benzo[*d*]thiazol-2'-yl)acetonitrile **4** (1.0 mmol, 0.17 g) and pyrimidine aldehyde **2** or **8** (1.0 mmol) was stirred at °25C for 10–15 min in ethanol (10 ml) which contained piperidine (2.0 mmol, 0.2 ml). The reaction was monitored by TLC. The formed solid was filtrated and washed with hexane (2 × 10 ml) to give the corresponding compounds **5** and **9a–d**.

4.4.2.1. (E)-2-(Benzo[*d*]thiazol-2'-yl)-3-(2'',4''-diaminopyrimidin-5''-yl)acrylonitrile (**5**). Yellow powder; yield 77 %; mp 280 °C; IR (KBr, cm⁻¹): 3395, 3307 (br, NH₂), 2101 (CN), 2733 (C-H aliphatic), 1565 (C=C); ¹H-NMR [DMSO-*d*₆, 400 MHz]: (δ, ppm) 6.86–6.88 (bs, 2H, NH₂, exchangeable with D₂O), 7.47 (t, 1H, H₅-benzothiazole, *J* = 8.0 Hz), 7.55 (t, 1H, H₆-benzothiazole, *J* = 8.0 Hz), 8.05 (d, 1H, H₄-benzothiazole, *J* = 8.0 Hz), 8.11 (d, 1H, H₇-benzothiazole, *J* = 8.0 Hz), 8.30 (brs, 2H, NH₂, exchangeable with D₂O), 8.52 (s, 1H, H₆-pyrimidine), 8.87 (olefinic H); ¹³C-NMR [DMSO-*d*₆, 100 MHz]: (δ, ppm) 106.4 (C5-pyrimidine), 110.1 (C2'), 112.2 (CN), 122.3 (C7-benzothiazole), 133.3 (C4-benzothiazole), 139.9 (C5-benzothiazole), 139.9 (C6-benzothiazole), 153.1 (C3'a-

benzothiazole), 160.0 (C6-pyrimidine), 161.5 (C3'b-benzothiazole), 162.9 (olefinic C), 164.5 (C4-pyrimidine), 164.8 (C2-benzothiazole), 167.1 (C2-pyrimidine); Anal. Calcd for C₁₄H₁₀N₆S: C, 57.13; H, 3.42; N, 28.55; S, 10.89; Found: C, 57.18; H, 3.33; N, 28.63; S, 10.96; Anal. Calcd for C₁₄H₁₀N₆S.2HBr: C, 36.86; H, 2.65; N, 18.42; S, 7.03; Found: C, 37.05; H, 2.45; N, 18.44; S, 7.05.

4.4.2.2. (E)-2-(Benzo[d]thiazol-2'-yl)-3-(2''-(dimethylamino)pyrimidin-5''-yl)acrylonitrile (**9a**). Yellow powder; yield 86 %; mp 251 °C; IR (KBr, cm⁻¹): 3408 (Ar-H *stret.*), 2926 (aliphatic C-H *stret.*), 2209 (CN), 1607 (C=C); ¹H-NMR [DMSO-*d*₆, 400 MHz]: (δ, ppm) 3.25 (s, 6H, 2CH₃), 7.47–7.56 (m, 2H, H_{5,6} benzothiazole), 8.01 (d, 1H, H₄ benzothiazole, *J* = 8.0 Hz), 8.10 (d, 1H, H₇ benzothiazole, *J* = 8.0 Hz), 8.17 (s, 1H, olefinic H), 9.02 (s, 2H, H_{4,6} pyrimidine); ¹³C-NMR [DMSO-*d*₆, 100 MHz]: (δ, ppm) 37.4 (CH₃), 100.5 (C2'), 115.3 (CN), 117.4 (C5-pyrimidine), 122.7 (C7-benzothiazole), 123.2 (C4-benzothiazole), 126.3 (C5-benzothiazole), 127.4 (C6-benzothiazole), 134.7 (C3'a-benzothiazole), 143.8 (C3'b-benzothiazole), 153.5 (olefinic C), 160.1 (C4,6-pyrimidine), 161.7 (C2-benzothiazole), 163.7 (C2-pyrimidine); Anal. Calcd for C₁₆H₁₃N₅S: C, 62.52; H, 4.26; N, 22.78; S, 10.43; Found: C, 62.57; H, 4.17; N, 22.86; S, 10.50; Anal. Calcd for C₁₆H₁₃N₅S.HBr: C, 49.49; H, 3.63; N, 18.04; S, 8.26; Found: C, 49.68; H, 3.43; N, 18.03; S, 8.27.

4.4.2.3. (E)-2-(Benzo[d]thiazol-2'-yl)-3-(2''-benzylaminopyrimidin-5''-yl)acrylonitrile (**9b**). Yellow powder; yield 78 %; mp 238 °C; IR (KBr, cm⁻¹): 3458 (NH), 3228 (aromatic C-H- *str.*), 2985 (C-H aliphatic), 2211 (CN), 1614 (C=C); ¹H-NMR [DMSO-*d*₆, 400 MHz]: (δ, ppm) 4.62–4.64 (d, 2H, CH₂, *J* = 8.0 Hz), 7.24–7.28 (m, 1H, benzylamine), 7.34–7.35 (m, 4H, benzylamine), 7.48 (t, 1H, H₅-benzothiazole, *J* = 8.0 Hz), 7.58 (t, 1H, H₆-benzothiazole, *J* = 8.0 Hz), 8.02 (d, 1H, H₄-benzothiazole, *J* = 8.0 Hz), 8.13 (d, 1H, H₇-benzothiazole), 8.17 (s, 1H, olefinic H), 8.92 (t, 1H, NH, exchangeable with D₂O), 9.47 (s, 2H, H_{4,6}-pyrimidine); ¹³C-NMR [DMSO-*d*₆, 100 MHz]: (δ, ppm) 44.6 (CH₂), 100.5 (C2'), 116.4 (CN), 117.4 (C5-pyrimidine), 122.8 (C7-benzothiazole), 123.2 (C4-benzothiazole), 126.4 (C5-benzothiazole), 127.3 (C6-benzothiazole), 127.6, 128.8, 134.5 (benzylamine), 139.6 (C3'a-benzothiazole), 143.8 (benzylamine), 153.4 (C3'b-benzothiazole), 160.6 (olefinic C), 160.9 (C4,6-pyrimidine), 162.4 (C2-benzothiazole), 163.9 (C2-pyrimidine); Anal. Calcd for C₂₁H₁₅N₅S: C, 68.27; H, 4.09; N, 18.96; S, 8.68; Found: C, 68.32; H, 4.01; N, 19.01; S, 8.75; Anal. Calcd for C₂₁H₁₅N₅S.HBr: C, 56.01; H, 3.58; N, 15.55; S, 7.12; Found: C, 56.20; H, 3.38; N, 15.56; S, 7.14.

4.4.2.4. (E)-2-(Benzo[d]thiazol-2'-yl)-3-(2''-morpholinopyrimidin-5''-yl)acrylonitrile (**9c**). Yellow powder; yield 80 %; mp 248 °C; IR (KBr, cm⁻¹): 3053 (aromatic C-H- *str.*), 2968 (CH-aliphatic), 2210 (CN), 1582 (C=C); ¹H-NMR [DMSO-*d*₆, 400 MHz]: (δ, ppm) 3.67–3.68 (m, 4H, morpholine), 3.83–3.84 (m, 4H, morpholine), 6.54 (t, 1H, H₅-benzothiazole, *J* = 8.0 Hz), 6.69 (d, 1H, H₄-benzothiazole, *J* = 8.0 Hz), 6.94 (t, 1H, H₆-benzothiazole, *J* = 8.0 Hz), 7.06 (d, 1H, H₇-benzothiazole, *J* = 8.0 Hz), 8.51 (s, 1H, olefinic H), 8.94 (s, 2H, H_{4,6}-pyrimidine); ¹³C-NMR [DMSO-*d*₆, 100 MHz]: (δ, ppm) 44.4, 66.4 (morpholine), 102.6 (C2'), 117.4 (CN), 119.5 (C5-pyrimidine), 124.8 (C7-benzothiazole), 125.4 (C4-benzothiazole), 128.4 (C5-benzothiazole), 129.5 (C6-benzothiazole), 136.8 (C3'a-benzothiazole), 145.9 (C3'b-benzothiazole), 155.7 (olefinic C), 162.3 (C4,6-pyrimidine), 163.8 (C2-

benzothiazole), 165.9 (C2-pyrimidine); Anal. Calcd for C₁₈H₁₅N₅OS: C, 61.87; H, 4.33; N, 20.04; S, 9.18; Found: C, 61.92; H, 4.24; N, 20.12; S, 9.25; Anal. Calcd for C₁₈H₁₅N₅OS.HBr: C, 50.24; H, 3.75; N, 16.27; S, 7.45; Found: C, 50.43; H, 3.55; N, 16.28; S, 7.46.

4.4.2.5. (E)-2-(Benzo[d]thiazol-2'-yl)-3-[2''-(p-chlorophenylamino)pyrimidin-5''-yl] acrylonitrile (**9d**). Crystallized from ethanol, orange powder; yield 83 %; mp 188 °C; IR (KBr, cm⁻¹): 3445 (br, NH), 3269 (aromatic C-H- *str.*), 3050 (C-H aliphatic), 2232 (CN), 1572 (C=C); ¹H-NMR [DMSO-*d*₆, 400 MHz]: (δ, ppm) 7.25 (d, 2H, *p*-chlorophenyl, *J* = 8.0 Hz), 7.40 (t, 1H, H₅-benzothiazole, *J* = 8.0 Hz), 7.57 (d, 1H, H₄-benzothiazole, *J* = 8.0 Hz), 7.84 (t, 1H, H₆- benzothiazole, *J* = 8.0 Hz), 8.03 (d, 1H, H₇- benzothiazole, *J* = 8.0 Hz), 8.26 (s, 1H, NH, exchangeable with D₂O), 8.44 (d, 2H, *p*-chlorophenyl, *J* = 7.8 Hz), 8.73 (s, 1H, olefinic H), 9.39 (s, 2H, H_{4,6}-pyrimidine); ¹³C-NMR [DMSO-*d*₆, 100 MHz]: (δ, ppm) 113.2 (C2'), 117.4 (CN), 118.3 (C5-pyrimidine), 119.2 (C7-benzothiazole), 126.9 (Ar-C, *p*-chlorophenyl), 127.8 (C4-benzothiazole), 130.6 (C5-benzothiazole), 131.0 (C6-benzothiazole), 131.3 (Ar-C, *p*-chlorophenyl), 132.1 (Ar-C, *p*-chlorophenyl), 136.3 (C3a'-benzothiazole), 137.9 (Ar-C, *p*-chlorophenyl), 138.6 (C3b'-benzothiazole), 147.1 (olefinic-C), 152.8 (C4,6-pyrimidine), 159.6 (C2-benzothiazole), 165.1 (C2-pyrimidine); Anal. Calcd for C₂₀H₁₂ClN₅S: C, 61.62; H, 3.10; N, 17.96; S, 8.22; Found: C, 61.67; H, 3.01; N, 18.03; S, 8.29; Anal. Calcd for C₂₀H₁₂ClN₅S.HBr: C, 51.03; H, 2.78; N, 14.88; S, 6.81; Found: C, 51.22; H, 2.58; N, 15.01; S, 6.91.

4.5. Synthesis of benzimidazole-pyrimidines

4.5.1. 2-(1*H*-Benzo[d]imidazol-2'-yl)acetonitrile (**11**). A mixture of *o*-phenylenediamine **10** (0.01 mol, 1.08 g) and ethyl cyanoacetate (0.01 mol, 1.7g) were refluxed in ethanol (30 mL) for 20 min. After cooling, the solution was extracted with ether (3 × 25 ml). The solvent was evaporated and the resultant solid product **11** was recrystallized from ethanol as a brown crystals; yield 75 %; mp 212 °C; ¹H-NMR [DMSO-*d*₆, 400 MHz]: (δ, ppm) 4.36 (s, 2H, CH₂), 5.17 (s, 1H, NH exchangeable with D₂O), 6.35 (m, 2H, H_{5,6}-benzimidazole), 6.47 (m, 2H, H_{4,7}-benzimidazole); ¹³C-NMR [DMSO-*d*₆, 100 MHz]: (δ, ppm) 22.8 (CH₂), 117.5 (CN), 122.8 (C4-benzimidazole), 123.1 (C7-benzimidazole), 126.1 (C5-benzimidazole), 127.0 (C6-benzimidazole), 135.5 (C3'-benzimidazole), 152.7 (C2-benzimidazole).

4.5.2. General synthetic procedure of (E)-2-(Benzo[d]imidazol-2'-yl)-3-arylacrylonitriles **12a-d**

A mixture of 2-(1*H*-benzo[d]imidazol-2'-yl)acetonitrile **11** (1.0 mmol, 0.16g) and pyrimidine aldehydes **8** (1.0 mmol) was stirred at 25°C for 10–15 min in ethanol (10.0 ml) that contained piperidine (2.0 mmol, 0.2 ml). The reactions were monitored by TLC, in order to verify the consumption of the precursors. The solid products were isolated by filtration and washed with a mixture of hexane/ethanol (7:3) to give the corresponding compounds **12a-d**.

4.5.2.1. (*E*)-2-(1*H*-Benzo[*d*]imidazol-2'-yl)-3-[2''-(dimethylamino)pyrimidin-5''-yl] acrylonitrile (**12a**). Orange crystals; yield 89 %; mp 154 °C; IR (KBr, cm⁻¹): 3439 (NH), 3307 (aromatic C-H-*str.*), 2860 (CH-aliphatic), 2395 (CN), 1616 (C=C); ¹H-NMR [DMSO-*d*₆, 400 MHz]: (δ, ppm) 3.21 (s, 6H, CH₃), 5.17 (s, 1H, NH exchangeable with D₂O), 6.54 (t, 1H, H₅-benzimidazole, *J* = 8.0 Hz), 6.68 (d, 1H, H₆-benzimidazole, *J* = 8.0 Hz), 6.93 (t, 1H, H₄- benzimidazole, *J* = 8.0 Hz), 7.05 (d, 1H, H₇-benzimidazole, *J* = 8.0 Hz), 8.49 (s, 1H, olefinic H), 8.89 (s, 2H, H_{4,6}-pyrimidine); ¹³C-NMR [DMSO-*d*₆, 100 MHz]: (δ, ppm) 37.26 (CH₃), 114.9 (C2'), 116.5 (C4,7-benzimidazole), 117.1 (CN), 119.0 (C5-pyrimidine), 127.5 (C5,6-benzimidazole), 135.9 (C3'-benzimidazole), 144.1 (C2-benzimidazole), 152.5 (olefinic C), 158.7 (C4,6-pyrimidine), 162.3 (C2-pyrimidine); Anal. Calcd for C₁₆H₁₄N₆: C, 66.19; H, 4.86; N, 28.95; Found: C, 66.24; H, 4.77; N, 29.03; Anal. Calcd for C₁₆H₁₄N₆.HBr: C, 51.77; H, 4.07; N, 22.64; Found: C, 51.96; H, 3.87; N, 22.66.

4.5.2.2. (*E*)-2-(1*H*-Benzo[*d*]imidazol-2'-yl)-3-[2''-(benzylamino)pyrimidin-5''-yl]acrylonitrile (**12b**). Light brown powder; yield 81 %; mp 152 °C; IR (KBr, cm⁻¹): 3471 (br, NH), 3367 (aromatic C-H-*str.*), 3226 (C-H aliphatic), 2207 (CN), 1614 (C=C); ¹H-NMR [DMSO-*d*₆, 400 MHz]: (δ, ppm) 4.59 (d, 2H, CH₂, *J* = 8Hz), 5.16 (s, 1H, NH exchangeable with D₂O), 6.53 (t, 1H, H₅-benzimidazole, *J* = 8.0 Hz), 6.67 (d, 1H, H₆-benzimidazole, *J* = 8.0 Hz), 6.93 (t, 1H, H₄-benzimidazole, *J* = 8.0 Hz), 7.03 (d, 1H, H₇- benzothiazole, *J* = 8.0 Hz), 7.22–7.25 (m, 1H, benzylamine), 7.29–7.33 (m, 4H, benzylamine), 8.36 (t, 1H, NH, exchangeable with D₂O), 8.46 (s, 1H, olefinic H), 8.88 (s, 2H, H_{4,6}-pyrimidine); ¹³C-NMR [DMSO-*d*₆, 100 MHz]: (δ, ppm) 44.5 (CH₂), 114.9 (C2'), 116.5 (C4,7-benzimidazole), 117.2 (CN), 120.3 (C5-pyrimidine), 127.1 (C5,6-benzimidazole), 127.5-135.9 (Ar-C, benzylamine), 140.2 (C3'-benzimidazole), 144.1 (C2- benzimidazole), 152.5 (olefinic C), 159.1 (C4,6-pyrimidine), 163.1 (C2-pyrimidine); Anal. Calcd for C₂₁H₁₆N₆: C, 71.58; H, 4.58; N, 23.85; Found: C, 71.63; H, 4.49; N, 23.93; Anal. Calcd for C₂₁H₁₆N₆.HBr: C, 58.21; H, 3.95; N, 19.40; Found: C, 58.41; H, 3.75; N, 19.39.

4.5.2.3. (*E*)-2-(1*H*-Benzo[*d*]imidazol-2'-yl)-3-(2''-morpholinopyrimidin-5''-yl)acrylonitrile (**12c**). Yellow powder; yield 84 %; mp 176 °C; IR (KBr, cm⁻¹): 3464 (br, NH), 3365 (aromatic C-H *str.*), 2967 (C-H aliphatic), 2331 (CN), 1604 (C=N); ¹H-NMR [DMSO-*d*₆, 400 MHz]: (δ, ppm) 3.67 (m, 4H, morpholine), 3.83 (m, 4H, morpholine), 5.20 (s, 1H, NH exchangeable with D₂O), 6.54 (t, 1H, H₅-benzimidazole, *J* = 8.0 Hz), 6.69 (d, 1H, H₆-benzimidazole, *J* = 8.0 Hz), 6.94 (t, 1H, H₄-benzimidazole, *J* = 8.0 Hz), 7.06 (d, 1H, H₇-benzimidazole, *J* = 8.0 Hz), 8.51 (s, 1H, olefinic H), 8.93 (s, 2H, H_{4,6}-pyrimidine); ¹³C-NMR [DMSO-*d*₆, 100 MHz]: (δ, ppm) 44.4, 66.4 (morpholine), 114.9 (C2'), 116.5 (C4,7-benzimidazole), 117.1 (CN), 120.1 (C5-pyrimidine), 127.6 (C5,6-benzimidazole), 135.7 (C3'-benzimidazole), 144.2 (C2-benzimidazole), 152.5 (olefinic C), 158.9 (C4,6-pyrimidine), 161.7 (C2-pyrimidine); Anal. Calcd for C₁₈H₁₆N₆O: C, 65.05; H, 4.85; N, 25.29; Found: C, 65.10; H, 4.76; N, 25.37; Anal. Calcd for C₁₈H₁₆N₆O.HBr: C, 52.31; H, 4.15; N, 20.34; Found: C, 52.51; H, 3.95; N, 20.36.

4.5.2.4. (*E*)-2-(1*H*-Benzo[*d*]imidazol-2'-yl)-3-(2''-(*p*-chlorophenyl)amino)pyrimidin-5''-yl) acrylonitrile (**12d**). Orange powder; yield 87 %; mp 258 °C; IR (KBr, cm⁻¹): 3446 (br, NH), 3350 (aromatic C-H-*str.*), 3023 (C-H aliphatic), 2260 (CN), 1606 (C=N); ¹H-NMR [DMSO-*d*₆, 400 MHz]: (δ, ppm) 5.47 (s, 1H, NH exchangeable with

D₂O), 6.58 (t, 1H, H₅-benzimidazole, $J = 8.0$ Hz), 6.74 (d, 1H, H₆-benzimidazole, $J = 8.0$ Hz), 7.02 (t, 1H, H₄-benzimidazole, $J = 8.0$ Hz), 7.21(d, 1H, H₇-benzimidazole, $J = 8.0$ Hz), 7.62 (d, 2H, *p*-Chlorophenyl, $J = 7.8$ Hz), 7.98 (s, 1H, NH, exchangeable with D₂O), 8.46 (d, 2H, *p*-Chlorophenyl, $J = 7.8$ Hz), 8.78 (s, 1H, olefinic H), 9.44 (s, 2H, H_{4,6}-pyrimidine); ¹³C-NMR [DMSO-*d*₆, 100 MHz]: (δ , ppm) 115.4 (C2'), 116.3 (C4,7-benzimidazole), 117.3 (CN), 123.4 (C5-pyrimidine), 129.1(C5,6-benzimidazole) 129.4–135.9 (Ar-C, *p*-chlorophenyl), 136.7 (C3' -benzimidazole), 145.2 (C2-benzimidazole), 150.9 (olefinic C), 157.7 (C4,6-pyrimidine), 163.1 (C2-pyrimidine); Anal. Calcd for C₂₀H₁₃ClN₆: C, 64.43; H, 3.51; N, 22.54; Found: C, 64.48; H, 3.42; N, 22.62; Anal. Calcd for C₂₀H₁₃ClN₆.HBr: C, 52.94; H, 3.11; N, 18.52; Found: C, 53.13; H, 2.91; N, 18.51.

4.6. Salt formation

Compounds **5**, **9a-d** and **12a-d** were dissolved in a minimal amount of methanol and treated with excess hydrobromic acid to form the hydrobromide salt. The salt was collected, washed with diethyl ether, and dried.

4.7. Antibacterial activity

4.7.1. Medium

The antibacterial assay was performed using the well diffusion method for all compounds **5**, **9a-d** and **12a-d**. Mueller Hinton agar (38.0 g of Mueller Hinton Agar in 1000 mL of distilled water) was prepared and autoclaved. It was poured into the petri dishes and solidified at °25C. The bacterial strains (10⁶ cells/ml) were introduced in the plates using pipettes and hockey sticks to spread on the agar. For well diffusion, well were made, and all the compounds were poured individually into the well (50 μ l/well). It was then incubated at 37 °C for 24–48 hours. The bacterial inhibition was determined by measuring the diameter of the inhibition zone (mm) using a transparent scale. Antibiotic (amoxicillin 5.0 mg/ml) was then used as a positive control at 50 μ l/well.

4.7.2. Test microorganisms

Two Gram-positive bacteria, namely, *Staphylococcus aureus* (ATCC-25923) and *Bacillus subtilis* (ATCC 6633) and two Gram-negative bacteria, namely, *Escherichia coli* (ATCC-25922) and *Pseudomonas aeruginosa* (ATCC-27853) were used to determine antibacterial activity.

4.7.3. Minimum inhibitory concentration (MIC)

Compounds **5**, **9a-d** and **12a-d** were serially diluted with autoclaved sterile distilled water and examined from lower to higher dilution to find the MIC. Serially diluted compounds (100 μ l) were added to sterile nutrient broth (900 μ l). A Control test-tube containing only medium (nutrient broth medium) was used to confirm the sterility of the medium bacterial cultures. Bacterial suspension (10 μ l) containing 10⁵ cells/ml was inoculated into all tubes. All of the test tubes were incubated at 37±1°C and observed for bacterial growth for 24 hours for MIC determination. After incubation, for 24 hours, the test tube with no visible growth of the microorganism was taken to represent the MIC value of the sample in μ g/ml. Triplicates of each tested compound were performed, and the average of the results was taken.

4.7.4. Minimum inhibitory concentration (MIC) for combination of amoxicillin (MIC) with **5** and **12d**

The minimal inhibitory concentration (MIC) of an antimicrobial compound is the lowest (i.e. minimum) concentration of the antimicrobial compound that inhibits a given bacterial strain. Compounds (amoxicillin, amoxicillin with **5** and **12d**) were serially diluted with autoclaved sterile distilled water and examined from lower to higher dilutions to find the MIC. Serially diluted compounds (100 μ l) were added to sterile nutrient broth (900 μ l). A Control test-tube containing only medium (nutrient broth medium) was used to confirm the sterility of the medium bacterial cultures. Bacterial suspension (10 μ l) containing 10^5 cells/ml was inoculated into all tubes. All of the test tubes were incubated at $37\pm 1^\circ\text{C}$ and observed for bacterial growth for 24 hours for MIC determination. After incubation, for 24 hours, the test tube with no visible growth of the microorganism was taken to represent the MIC value of the sample in $\mu\text{g/ml}$.

4.7.5. Transmission electron microscopy analysis

Transmission electron microscopy (TEM) was used to evaluate the morphological changes in *E. coli* after treatment with compound **5**. Treated bacterial and control cells were processed by the same procedure for all techniques. Upon incubation, the pellets obtained after centrifugation were fixed in Carnovsky's fixative at 25°C for 3–4 hours with a mixture containing 2 % paraformaldehyde and 2.5% glutaraldehyde. The bacteria were then washed three times with 0.1 M phosphate buffer, pH 7.2 for 5 minutes. The bacteria were then centrifuged at 10,000 rpm in an Eppendorf tube for 15 minutes. The bacterial pellet was resuspended in 1.0 ml of phosphate buffer and then adsorbed on formvar carbon coated supports, Agar 200-mesh copper grids by floating the grids on a drop of bacterial isolate. The bacteria on grids were stained by submerging the grids for 5 minutes in 12 % (w/v) aqueous uranyl acetate, and were then rinsed with Milli-Q water three times. The grids were examined and photographed under a Philips CM10 transmission electron microscope using an accelerating voltage of 80 kV. Images were taken at different magnifications [31–33].

4.8. Docking studies using penicillin-binding protein receptor and β -lactamase enzyme

The *E. coli* penicillin-binding protein 4 (PBP4) crystal structure used in this docking study was downloaded from the protein data bank [34] (PDB ID: 2EX8 [35]). The crystal structure of the *E. coli* β -lactamase enzyme used in this docking study was downloaded from the protein data bank [34] (PDB ID: 1FQG [36]). The crystal structure was checked by MOE using the protein preparation module [37], with a few corrections to the structure. All water and ligand molecules were removed. It was then processed via the Protein Preparation Wizard [38, 39] in the Maestro software [40], mainly to establish partial charges on each atom using OPLS force field and to assign a protonation state on each ionizable group. The whole structure was relaxed via conducting restrained minimization with an RMSD limit up to 0.3 Å. The binding pocket was identified with co-crystallized ligand (penicillin G).

All ligands were created using MOE [28] which was also used to generate the dominant ionization state for each ionizable functional group. Ligands were then prepared using the LigPrep module [41] in the Maestro program [40] in order to give partial charges to ligand atoms and to generate a single low-energy conformation for each ligand using the OPLS force field. Next, all ligands were covalently docked into the previously prepared

binding site using the Covalent Docking module [42] in Maestro, with the thorough pose predication algorithm employed for conformational sampling. Two main reaction types were set: β -lactam addition and conjugate addition to nitrile-activated alkene, both of which were set to react with the Ser62 side chain. Pose refinement and scoring were kept as default. Docked poses were scored by taking the average of two GlideScore [43, 44] values, Glide docking score “pre-reacted” and a score-in-place “post-reacted” calculation, for the final docked pose [42]. GlideScore is an empirical scoring function that approximates the ligand-binding free energy. It has many terms, including force field (electrostatic, van der Waals) contributions and terms rewarding or penalizing interactions known to influence ligand binding [44].

4.9. Spectroscopic studies

4.9.1. Standard solutions

4.9.1.1. Phosphate buffer solution

A 0.01 M phosphate buffer solution (pH = 7.4) was prepared by dissolving appropriate amounts of H_3PO_4 and KOH in 1.0 L of deionized water. The pH was adjusted on glass electrode using the standard procedure for buffer preparation.

4.9.1.2. β -Lactamase enzyme solution

β -lactamase enzyme solution (1×10^{-6} M) was prepared by dissolving an appropriate amount of the enzyme in the phosphate buffer (pH 7.4). The stock solution was stored at 4 °C for 24 hours.

4.9.1.3. Pyrimidine acrylonitrile derivatives solutions

Stock solutions of compounds **5** and **12d** were prepared by dissolving appropriate amounts of each compound in the phosphate buffer (pH 7.4) to final concentrations of 6×10^{-5} M.

4.9.2. UV-Vis measurements

UV-vis absorption spectra were recorded using 6×10^{-5} M of compounds **5** and **12d** and incremental addition of enzyme solution (1×10^{-6} M, 10 μ l) in phosphate buffer, pH 7.4. The measurement ranged between 200 and 700 nm at the different enzyme-compound ratios and were recorded three minutes after incubation to permit equilibrium between the species. Titration stopped at saturation, when no change in absorbance intensity was observed.

4.9.3. Fluorescence measurements

Interactions of pyrimidine acrylonitrile derivatives **5** and **12d** with β -lactamase enzyme were followed fluorimetrically at 443 and 456 nm as λ_{max} of emission using excitation λ_{max} of 280 and 290 nm, respectively. A fixed concentration of each compound was titrated with the incremental addition of enzyme (10 μ l) in phosphate buffer, pH 7.4 and the fluorescence measurements were performed keeping the excitation and emission band slit width of 5–10 nm, after allowing three minutes' equilibration for each enzyme addition, and scanned for

fluorescence spectra in the range 300–600 nm. Titrations were stopped at saturation when no change in fluorescence intensity was observed. A fluorescence-free quartz cell of 1 cm path length was used.

4.9.4. Circular dichroism measurements

Circular dichroism spectroscopy was used to confirm the results obtained by UV and fluorescence spectroscopies. Interactions between pyrimidine acrylonitrile derivatives **5** and **12d** with β -lactamase enzyme were followed by adding successive amounts (6×10^{-5} M) to 1.0 mL of β -lactamase enzyme in phosphate buffer, pH 7.4. The CD spectra were recorded at $^{\circ}25\text{C}$ in the wavelength range of 200–700 nm, at a speed of 50 nm/min and bandwidth of 1 nm. Each spectrum was averaged from three successive accumulations. All CD spectra were auto baseline-corrected against blank solutions. Before use, the optical chamber of the CD spectrometer was deoxygenated with dry nitrogen and was held under nitrogen atmosphere during the measurements. UV-vis, fluorescence and CD signals were corrected for dilution effects.

4.9.5. NMR studies of the interaction between β -lactamase and **12d**

Compound **12d** (10 mg) was dissolved in 0.3 ml of deuterium oxide (D_2O , Merck) in an NMR tube, and the ^1H -NMR spectrum was immediately recorded as a zero-time reference. The β -lactamase solution in 0.3 ml of 0.1 M phosphate buffer was added to the NMR tube, and the ^1H -NMR spectrum was recorded at 37°C after 60 min.

Acknowledgment

The authors wish to acknowledge the significant financial support of UAE University, Research Affairs Sector (grant no. 31S030-1156-02-02-10).

Appendix A. Supplementary data

Supplementary data related to this article can be found at <https://1drv.ms/b/s!Aoxf511qpqQthX9jJS6H0k92Mm1O>

References

- [1] J. V. Carlet J, S. Harbarth, A. Voss, H. Goossens, D. Pittet, Ready for a world without antibiotics? The Pensières Antibiotic Resistance Call to Action, *Antimicrobial Resistance and Infection Control*. 1 (2012) 1-13.
- [2] T. L. Gilchrist., third ed., Addisone Wesley Longman, Ltd., England, 1998.
- [3] D.Q. Shi, Rong, Shao-Feng, Dou, Guo-Lan, Efficient Synthesis of 2-Arylbenzothiazole Derivatives with the Aid of a Low-Valent Titanium Reagent, *Synthetic Communications*. 40 (2010) 2302-2310.
- [4] D. Lednicer, Wiley & Sons, New York, 1998.
- [5] Y.S. Tong, J.J. Bouska, P.A. Ellis, E.F. Johnson, J. Levenson, X.S. Liu, P.A. Marcotte, A.M. Olson, D.J. Osterling, M. Przytulinska, L.E. Rodriguez, Y. Shi, N. Soni, J. Stavropoulos, S. Thomas, C.K. Donawho, D.J. Frost, Y. Luo, V.L. Giranda, T.D. Penning, Synthesis and Evaluation of a New Generation of Orally Efficacious Benzimidazole-Based Poly(ADP-ribose) Polymerase-1 (PARP-1) Inhibitors as Anticancer Agents, *Journal of Medicinal Chemistry*. 52 (2009) 6803-6813.

- [6] Y. F. Li, G. F. He Wang, P. L. Huang, W. G. Zhu, F. H. Gao, H. Y. Tang, W. Luo, Y. Feng, C. L. Shi, L. P. Ren, Y. D. Lu, W. Zuo, J. P., Synthesis and Anti-Hepatitis B Virus Activity of Novel Benzimidazole Derivatives, *Journal of Medicinal Chemistry*. 49 (2006) 4790-4794.
- [7] H. K. Achar KC, HR. Seetharamareddy, In-vivo analgesic and anti-inflammatory activities of newly synthesized benzimidazole derivatives, *European Journal of Medicinal Chemistry*. 45 (2010) 2048-2054.
- [8] B. A. Le Sann C, J. Mann, H. van den Berg, M. Gunaratnam, S. Neidle, New mustard-linked 2-aryl-bisbenzimidazoles with anti-proliferative activity, *Organic and Biomolecular Chemistry*. 4 (2006) 1305-1312.
- [9] B. M. Kálai T, A. Szabó, G. Gulyás, J. Jeko, B. Sümegi, K. Hideg, New Poly(ADP-ribose) Polymerase-1 Inhibitors with Antioxidant Activity Based on 4-Carboxamidobenzimidazole-2-ylpyrroline and -tetrahydropyridine Nitroxides and Their Precursors, *Journal of Medicinal Chemistry*. 52 (2009) 1619-1629.
- [10] D. D. Werner W.K.R Mederski, A. Soheila, G. Johannes, C. Bertram, T. Christos, Halothiophene benzimidazoles as P1 surrogates of inhibitors of blood coagulation factor Xa, *Bioorganic & Medicinal Chemistry Letters*. 14 (2004) 3763-3769.
- [11] M. S. Prabal Bandyopadhyay, S. Ponmariappan, S. Arti, S. Pratibha, A.K. Srivastava, M.P. Kaushik, Exploration of in vitro time point quantitative evaluation of newly synthesized benzimidazole and benzothiazole derivatives as potential antibacterial agents, *Bioorganic & Medicinal Chemistry Letters*. 21 (2011) 7306-7309.
- [12] R. R. P. Seenaiiah D, G. Mallikarjuna Reddy, A. Padmaja, V. Padmavathi, N. Siva Krishna, Synthesis, antimicrobial and cytotoxic activities of pyrimidinyl benzoxazole, benzothiazole and benzimidazole, *European Journal of Medicinal Chemistry*. 77 (2014) 1-7.
- [13] S.M. Shaveta, Palwinder Singh, Hybrid molecules: The privileged scaffolds for various pharmaceuticals, *European Journal of Medicinal Chemistry*. 124 (2016) 500-536.
- [14] Y. I. Yildiz-Oren I, E. Aki-Sener, N. Ukarturk, Synthesis and structure-activity relationships of new antimicrobial active multisubstituted benzazole derivatives, *Eur. J. Med. Chem*. 39 (2004) 291.
- [15] W.Y. Zhou C. H., Recent researches in triazole compounds as medicinal drugs, *Curr Med Chem*. 19 (2012) 239-280
- [16] T. W. Heng S, S. Hautmann, K. Kuan, D.S. Pedersen, M. Pietsch, M. Gütschow, A.D. Abell, New cholesterol esterase inhibitors based on rhodanine and thiazolidinedione scaffolds, *Bioorg. Med. Chem*. 19 (2011) 7453-7463.
- [17] M. N. A. Chrostowska, T. X, A. Dargelos, S. Khayar, A. Gracia, J-C. Guillemin, Beta-heterosubstituted acrylonitriles-electronic structure study by UV-photoelectron spectroscopy and quantum chemical calculations, *J. Phys. Chem*. 113 (2009) 2387.
- [18] C. D. Quiroga J, B. Insuasty, R. Abonía, M. Noguerras, J. Cobo, Y. Vásquez, M. Gupta, M. Derita, S. Zacchino, Synthesis and evaluation of novel E-2-(2-thienyl)- and Z-2-(3-thienyl)-3-arylacrylonitriles as antifungal and anticancer agents, *Arch. Pharm*. 340 (2007) 603.
- [19] E. T. Orge, J. V. Kelly, J. P. Dency, Q. Jairo, O. Alejandro, Microwave-Assisted Synthesis under Solvent-Free Conditions of (E)-2-(Benzo[d]thiazol-2-yl)-3-arylacrylonitriles, *J. Braz. Chem. Soc*. 22 (2011) 2396-2402.
- [20] M. D. Kamal, A. F. Abdelbasset, F. A. Bakr, 1H-Benzimidazole-2-acetonitriles as Synthons in Fused Benzimidazole Synthesis, *J. Heterocyclic Chem*. 47 (2010) 243.

- [21] A. M. U. Demirayak S, A. Cağrı Karaburun, Synthesis and anticancer and anti-HIV testing of some pyrazino[1,2-a]benzimidazole derivatives, *Eur J Med Chem.* 37 (2002) 255.
- [22] P. K. S. Gulshan Kumar, S. Silky, S. Simranjeet, Synthesis and antimicrobial studies of fused heterocycles 'pyrimidobenzothiazoles' *Journal of Chemical and Pharmaceutical Research.* 7 (2015) 710-714.
- [23] S. Leekha, Christine L. Terrell, and Randall S. Edson, *General Principles of Antimicrobial Therapy*, Mayo Clinic Proceedings. 86 (2011) 156-167.
- [24] M. C. Worthington RJ, Overcoming Resistance to β -Lactam Antibiotics., *The Journal of organic chemistry.* 78 (2013) 4207-4213.
- [25] S. V. Bajaksouzian M.A, M.R. Jacobs, P. C. Appelbaum, Activities of levofloxacin, ofloxacin, and ciprofloxacin, alone and in combination with amikacin, against acinetobacters as determined by checkerboard and time-kill studies, *Antimicrob. Agents Chemother.* 41 (1997) 1073–1076.
- [26] B. Li, S. C. Cardinale, M. M. Butler, R. Pai, J. E. Nuss, N. P. Peet, S. Bavari, T. L. Bowlin, Time-dependent botulinum neurotoxin serotype A metalloprotease inhibitors, *Bioorganic & Medicinal Chemistry.* 19 (2011) 7338-7348.
- [27] D. Plewczynski, M. Lazniewski, R. Augustyniak, K. Ginalski, Can we trust docking results? Evaluation of seven commonly used programs on PDBbind database, *Journal of Computational Chemistry.* 32 (2011) 742-755.
- [28] K. Undheim, T. Benneche, Pyrimidines and their Benzo Derivatives, in: A.R.K.W.R.F.V. Scriven (Ed.) *Comprehensive Heterocyclic Chemistry II*, Pergamon, Oxford, 1996, pp. 93-231.
- [29] S. M. P. Kelly, N. C, *The Use of Circular Dichroism in the Investigation of Protein Structure and Function*, *Current Protein and Peptide Science.* 1 (2000) 349-384.
- [30] L. DM, Enzymatic assay of beta-lactamase using circular dichroism spectropolarimetry., *Anal Biochem.* 247 (1997) 389-393.
- [31] F.S. Sjostrand, A method to improve contrast in high resolution electron microscopy of ultrathin tissue sections, *Exp.Cell Res*, 10 (1956) 657-664.
- [32] E.S. Reynolds, The use of Lead Citrate at high pH as an electron- opaque stain in electron microscopy, *J.Cell Biol*, 17 (1963) 208-212.
- [33] M.J. Karnovsky, A formaldehyde-glutaraldehyde fixative of high osmolarity for use in electron microscopy, *J.Cell Biol*, 27 (1965) 137.
- [34] R. A. Jones, Pyrroles and their Benzo Derivatives: (ii) Reactivity, in: A.R.K.W. Rees (Ed.) *Comprehensive Heterocyclic Chemistry*, Pergamon, Oxford, 1984, pp. 201-312.
- [35] E. D. Sauvage, A. Fraipont, C. Joris, M. Herman, R. Rocaboy, M. Schloesser, M. Dumas, J. Kerff, F. Nguyen-Disteche, M. Charlier P, Crystal Structure of Penicillin-Binding Protein 3 (PBP₃) from *Escherichia coli*, *PLoS ONE.* 9 (2014) 98042.
- [36] N. C. J. Strynadka, H. Adachi, S. E. Jensen, K. Johns, A. Sielecki, C. Betzel, K. Sutoh, M. N. G. James, Molecular structure of the acyl-enzyme intermediate in [β]-lactam hydrolysis at 1.7 Å resolution, *Nature.* 359 (1992) 700-705.
- [37] Graphical contents list, *Tetrahedron Letters*, 53 (2012) 2925-2935.

- [38] X. Wang, A. Song, S. Dixon, M. J. Kurth, K. S. Lam, Facile solid phase synthesis of 1,2-disubstituted-6-nitro-1,4-dihydroquinazolines using a tetrafunctional scaffold, *Tetrahedron Letters*. 46 (2005) 427-430.
- [39] G. Madhavi Sastry, M. Adzhigirey, T. Day, R. Annabhimoju, W. Sherman, Protein and ligand preparation: parameters, protocols, and influence on virtual screening enrichments, *Journal of Computer-Aided Molecular Design*. 27 (2013) 221-234.
- [40] F. Shi, Y. Deng, T. SiMa, H. Yang, A novel $ZrO_2-SO_4^{2-}$ supported palladium catalyst for syntheses of disubstituted ureas from amines by oxidative carbonylation, *Tetrahedron Letters*. 42 (2001) 2161-2163.
- [41] S. Lü, W. Zheng, L. Ji, Q. Luo, X. Hao, X. Li, F. Wang, Synthesis, characterization, screening and docking analysis of 4-anilinoquinazoline derivatives as tyrosine kinase inhibitors, *European Journal of Medicinal Chemistry*. 61 (2013) 84-94.
- [42] K. Zhu, K. W. Borrelli, J. R. Greenwood, T. Day, R. Abel, R. S. Farid, E. Harder, Docking Covalent Inhibitors: A Parameter Free Approach To Pose Prediction and Scoring, *Journal of Chemical Information and Modeling*. 54 (2014) 1932-1940.
- [43] N. Vasdev, P. N. Dorff, J. P. O'Neil, F. T. Chin, S. Hanrahan, H. F. VanBrocklin, Metabolic stability of 6,7-dialkoxy-4-(2-, 3- and 4-[^{18}F]fluoroanilino)quinazolines, potential EGFR imaging probes, *Bioorganic & Medicinal Chemistry*. 19 (2011) 2959-2965.
- [44] T. A. Halgren, R. B. Murphy, R. A. Friesner, H. S. Beard, L. L. Frye, W. T. Pollard, J. L. Banks, Glide: A New Approach for Rapid, Accurate Docking and Scoring. 2. Enrichment Factors in Database Screening, *Journal of Medicinal Chemistry*. 47 (2004) 1750-1759.

Highlights

- Novel benzazole-pyrimidines with antimicrobial properties are synthesized.
- Compounds **5** and **12d** are highly active in both *in vitro* and molecular docking studies.
- Physical studies of compounds **5**, **12d** with β -lactamase enzyme is described.
- *In-vitro* study showed that a combination of the new analogues and Amoxicillin indicates a synergistic effect.
- Docking study and TEM suggest the membrane disruption action of **5**.